https://doi.org/10.20965/ijat.2017.p0645

Paper:

Analysis and Control of Pouring Ladle with Weir for Sloshing and Volume-Moving Vibration in Pouring Cut-Off Process

Atsushi Ito*, **Ryosuke Tasaki***, **Makio Suzuki****, **and Kazuhiko Terashima***

*Department of Mechanical Engineering, Toyohashi University of Technology
1-1 Hibarigaoka, Tempaku, Toyohashi, Aichi 441-8580, Japan
†Corresponding author, E-mail: a_ito@syscon.me.tut.ac.jp
**Sintokogio, Ltd., Aichi, Japan

[Received January 15, 2017; accepted April 14, 2017]

This paper presents analysis results of molten metal vibration for the pouring ladle of an automatic pouring system and proposes vibration suppression control during backward tilting of the ladle in the pouring cut-off process. The pouring ladle has a weir to avoid contamination of the molten metal. The weir separates the interior of the ladle into a body side and a nozzle side. First, weir effects on flow behavior are analyzed by comparing ladles with and without weirs using computational fluid dynamics simulations. In this analysis, a trapezoidal shaped input is designed as a backward tilting velocity. As a result, molten metal in the ladle with weir shows not only sloshing but also moving-volume vibration at the weir opening area. Secondly, the center points of the tilting motion are each verified by residual vibrations using FFT analysis. The frequencies of vibrating elements are nearly identical; however, analysis results show that the sloshing magnitude varies with changing center point of the tilting motion. In addition, effects of weir position and opening area on peak frequencies are analyzed. Each condition affects a frequency of moving-volume vibration. In addition, weir position changes sloshing frequencies at both body side and nozzle side of the pouring ladle. Finally, the suppression control input for each vibration is designed using the Input Shaping control approach. Design parameters for the control input were identified from residual vibrations, and assumed to be a second-order lag system. The effectiveness of the proposed suppression control input is verified by comparison with the non-controlled case.

Keywords: casting industry, automatic pouring system, sloshing, volume-moving vibration, vibration suppression control

1. Introduction

Casting, one of the metal processing methods, by which molten metal is poured into molds to form desired shapes, is a fundamental technology to support the automobile, machine tool, and aircraft industries. While casting is

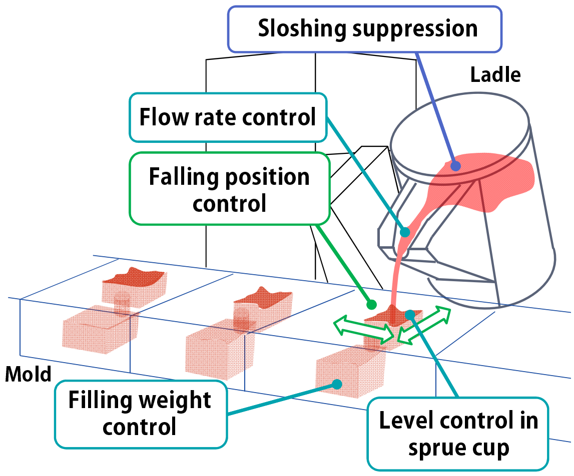

Fig. 1. Tilting-type automatic pouring system.

advantageous in forming complex shapes or processing abrasion resistant alloys that are hard to machine, casting sites are considered so-called 3D (dirty, dangerous, and difficult) workplaces. In particular, molten metal pouring processes, where workers are exposed to 1300°C molten metal, place a heavy burden on workers. To cope with the above-mentioned situation, automatic pouring systems have been developed [1–4]. Typical automatic pouring systems include a tilting type [5, 6], stopper type [7], and a pressure type [8]. The automatic tilting pouring system shown in **Fig. 1** pours molten metal into molds by tilting a holding pot, called a ladle, with an actuator in a fashion similar to the manual process. While this system has advantages in making optimal use of skilled workers' know-how as well as in high maintainability due to its simple construction, it is difficult to control the molten metal flow. Therefore, in order to make best use of the above-mentioned advantages we need to resolve the difficulties with molten metal pouring control. Research and development was focused on the technologies for controlling the molten metal flows from a tilting-type pouring system.

In the tilting-type pouring system, when a ladle is transferred from the melting furnace to a target mold to pour molten metal into it, sloshing of the molten metal inside

© Fuji Technology Press Ltd. Creative Commons CC BY-ND: This is an Open Access article distributed under the terms of the Creative Commons Attribution-NoDerivatives 4.0 International License (http://creativecommons.org/licenses/by-nd/4.0/).

the ladle is sometimes excited by the pouring motion of the ladle. If such sloshing is excited, it can absorb dust and air on the molten metal surface which will contaminate the molten metal. If any residual vibrations remain on the molten metal surface after the backward tilting of the ladle, they could lead to some defects in products or to a longer processing time. The above-mentioned concerns necessitate sloshing control when transferring a ladle from the furnace to a mold for the pouring of molten metal.

The analysis of the sloshing phenomenon caused by the transferring of a liquid in a container is the subject of studies in both the fluid- and vibration-engineering fields, and vibration control is the subject of studies in the control engineering field. Grundelius et al. derived transfer acceleration inputs for practical vibration control by solving the optimization problem of minimizing energy with a linearized sloshing model in the process of packaging liquid containers [9]. Takahara et al. demonstrated the relationships between structural shapes/positions and their natural frequencies by the boundary element method and experiments on liquid containers with some columnar or partition plate structures inside [10, 11]. Katsube et al. gained high vibration-suppression effects by using both preview control and generalized predictive control for the liquid surface feedback system composed of ultrasonic sensors, on the assumption that sloshing is equivalent to a pendulum motion [12–14]. Kanazawa et al. conducted computational fluid dynamics (CFD) analyses of liquid motion inside beverage bottles in the beverage bottling process and optimized the motion curves in transferring bottles on a genetic algorithm [15]. Shibuya et al. clarified by the principal component analyses from the CFD analyses and experimental results, the relationship between the natural frequencies of sloshing, shapes/postures of liquid containers, and liquid volumes in liquid containers, and achieved vibration suppression control for varying postures and liquid volumes with adaptive notch filters, using the obtained characteristic formula [16].

If any vibrations occur when the molten metal is poured, the outflowing molten metal could fall in an unexpected trajectory, which could cause some defective products as well as lead to equipment being damaged, or accidents. In order to suppress vibrations of molten metal when being poured, Fukushima et al. examined the natural frequencies with the ladle in different postures and designed adaptive notch filters accordingly so that poured molten metal's falling positions could be stabilized [17]. The ladle could be tilted backwards at the actuator's maximum velocity to stop molten metal flows, or to cut off the molten metal pouring process. Terashima et al. derived control inputs that could achieve both vibration suppression and backward tilting motion with the Input Shaping control so that no residual vibrations should occur after the ladle's backward tilting [18].

The above-mentioned cases show that there are numerous studies available on sloshing-suppression control. Vibration suppression control in casting processes is intended for containers with comparatively simple shapes.

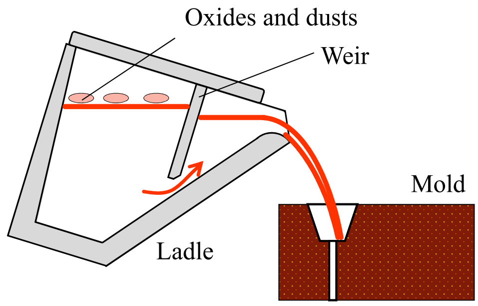

Fig. 2. Teapot shape ladle.

Many of the ladles used in actual automatic pouring systems have a weir inside as shown in **Fig. 2** [19]. The weir plays the role of preventing dust being absorbed in the molten metal supplied from the melting furnace, or oxides generated on the molten metal surface from entering the molds. There are some studies available on sloshing of liquid containers with multiple liquid surfaces [10], but their analytic formulae are too complicated to apply to sloshing control. In the tilting-type automatic pouring system, it is possible to arbitrarily set virtual rotation axes by synchronizing its front-back and lifting-lowering motions to the tilting motions [20]. When tilting a molten metal pouring system backwards, the center point of rotation depends on the specific system, thus there are no previous studies available on the comparison of liquid behaviors in containers with different centers of rotation. Moreover, as the weir is manually installed and its opening will become blocked with dust or oxides in the course of batch processing, it is essential to clarify any effects the weir's position, or opening areas, will have on casting operations.

In this study, we perform CFD analyses of sloshing and fluid behaviors that will occur in the process of cutting off the pouring of molten metal from an automatic pouring ladle with a weir inside in order to clarify the effects of the ladle's rotational positions, and the weir's positions and opening areas. We also study how to suppress sloshing using the vibration-suppression control approach.

2. CFD Analysis of Liquid Behavior in Ladle with Weir

Figure 3 shows the internal shape of the ladle that is analyzed in this study. The ladle, with the same internal shape and dimensions as one used in an actual automatic pouring system, comprises the cylindrical body and the narrow-mouth nozzle, and can hold 700 kg of molten metal. As an automatic pouring system has a tilting motor mounted near the ladle's center of gravity, the ladle model described in this section is designed to tilt around the axis shown in **Fig. 3**.

The initial conditions for the CFD analyses are described below. In this study, we use FLOW-3D (Flow Science Inc.) to analyze liquid flows inside a ladle [21, 22].

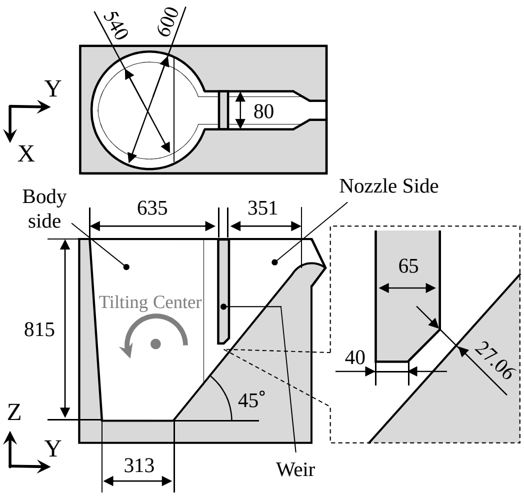

Fig. 3. Solid model of automatic pouring ladle with weir.

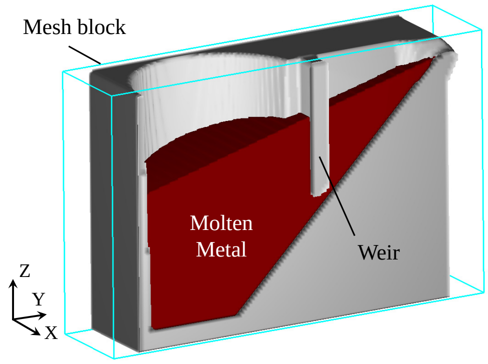

Fig. 4. 3D ladle model and mesh setting.

Table 1. Mesh parameters.

Block	Cell size [m]	Number of cells
X-direction	0.01	32
Y-direction	0.01	140
Z-direction	0.01	90
Total number of cells		403,200

In order to reduce the computational load, we use a three-dimensional (3D) ladle model halved in the X-direction as shown in **Fig. 4**. Meshes for the calculations are arranged in accordance with the halved size of the ladle, symmetric boundary conditions are set on the mesh surface that correspond to the center cross-section of the ladle, and continuous boundary conditions are set on the other five mesh surfaces. **Table 1** shows the cell size and the number of cells used in the calculations.

Figure 5 shows the backward tilting-motion velocity input used for the simulations. We have designed the velocity input as a trapezoidal waveform with a rising/falling acceleration of $\pm 40°/\text{s}^2$, a backward tilting velocity of $-7°/\text{s}$, and a backward tilting angle of $-5°$. The input design values were chosen with reference to the backward tilting motion of an actual pouring system. The calculation time was reduced by treating the ladle's motion as a non-inertial frame model that moves with gravity instead of letting it move in the simulation space [18]. The molten metal surface in a ladle is inclined before the ladle starts tilting backwards, as shown in **Fig. 4**. In this paper, the ladle's initial angle is set at 15° and the liquid volume inside the ladle is so designed as to be at a maximum in the condition where no liquid flows out of the nozzle.

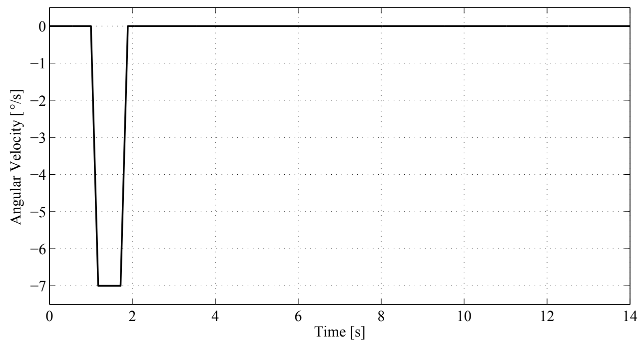

Fig. 5. Velocity input for backward tilting motion.

Table 2. Fluid properties of compact graphite iron.

Density of fluid [kg/m^3]	6337
Viscosity of fluid [Pa·s]	0.003202

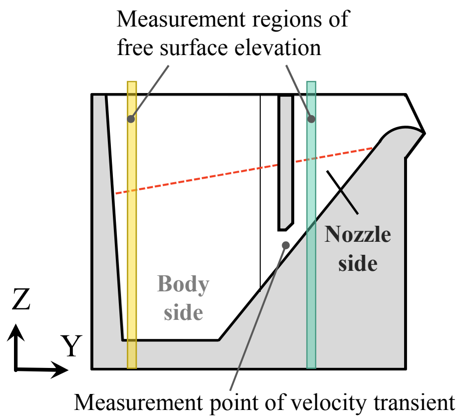

Fig. 6. Measurement regions and points for liquid vibration detection.

Table 2 lists the physical properties of the molten cast iron used in the simulations. We have set pressure conditions as incompressible, and Newtonian fluid as the viscosity characteristic for the analyses. As the actual pouring is a quick process, the analytical calculations take no account of any conditions for temperature changes such as heat conduction or solidification.

In order to evaluate the sloshing generated in a ladle, we have identified the regions where to detect liquid levels and the points where to detect flow velocities, as shown in **Fig. 6**. The liquid level measurement regions and the flow velocity measurement points are arranged on the symmetrical boundary of the meshes on the X-axis in order for

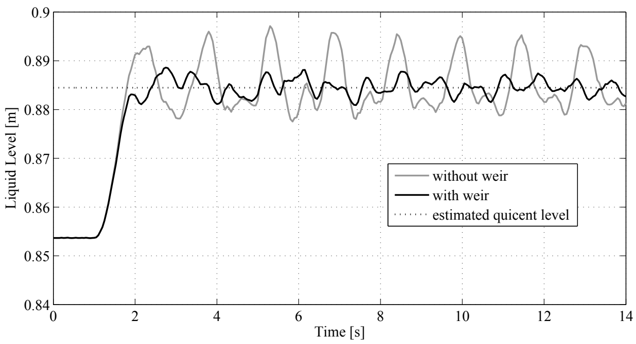

(a) Body side

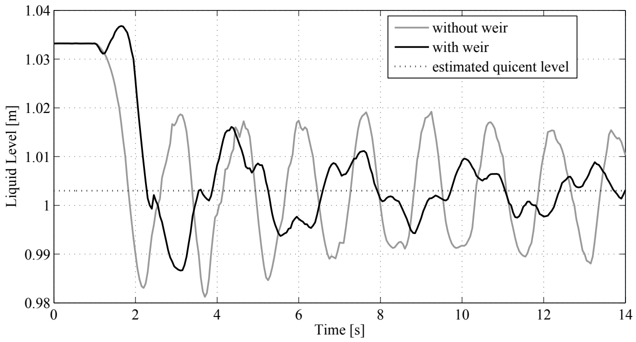

(b) Nozzle side

Fig. 7. Residual vibrations with and without a weir.

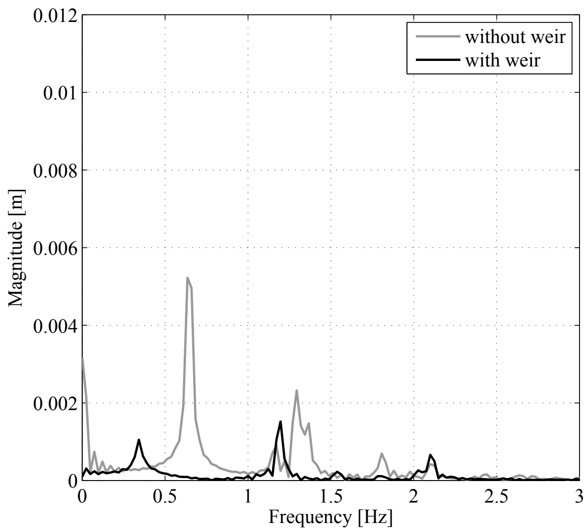

(a) Body side

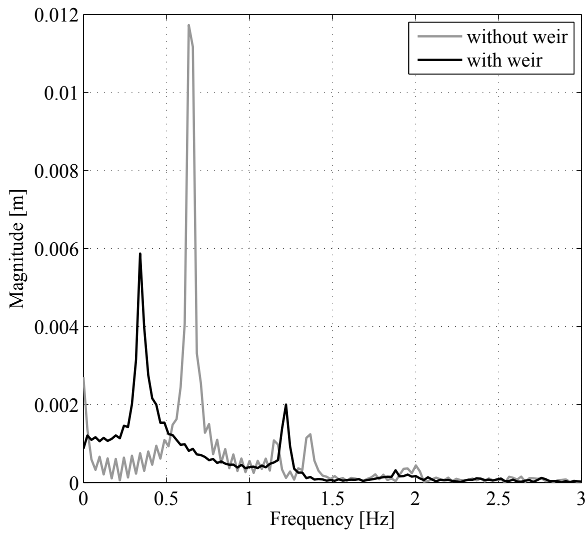

(b) Nozzle side

Fig. 8. FFT analysis results with and without a weir.

them to be detected in the ladle's center position. The liquid-level measurement regions are arranged approximately 0.003 m from the wall surface on the body side, and 0.002 m from the weir on the nozzle side. In a ladle with a weir, any liquid movement between the body and the nozzle will pass through the weir opening, so the flow velocity changes are measured at a point near the center of the opening where it is easier to check inflows and outflows of the liquid; the velocity component in the Y-axial direction is measured.

2.1. Comparison of Sloshing and Velocity Distributions with and Without a Weir

In this section, we discuss differences in liquid flows of ladles with and without weirs. To quantify such differences, we created a 3D ladle model with no weir (equivalent to the ladle in **Fig. 3** with no weir) and compared it with the original ladle shape by means of CFD analysis.

Figure 7 shows the changes in liquid levels, as measured in the regions set in **Fig. 6**, as absolute coordinate values in the simulation space. **Fig. 8** shows the FFT analysis results for the residual vibrations in **Fig. 7**. **Figs. 9** and **10** show the velocity distributions and vectors from 1–4 s after the start of the backward tilting of the ladles with and without weirs, respectively. The color maps are set for the range 0–0.4 m/s and the regions marked in red indicate liquid flows of 0.4 m/s or more.

As for the ladles without weirs, the velocity distributions in **Fig. 9** and the residual vibrations in **Fig. 7** show sustained sloshing after the end of the ladle's backward tilting motion. The velocity distributions show comparatively faster liquid flows on the nozzle side, which appears to be a result of the horizontal cross-sectional area on the nozzle side being significantly smaller than that on the body side, as can be clearly seen in **Fig. 3**. This decrease in the cross-sectional area increases the flow velocities when liquid moves in the ladle. The FFT analysis results in **Fig. 8** show peaks of 0.64 Hz due to 1st mode sloshing on the body side as well as on the nozzle side, but peaks of residual vibration amplitudes and frequency responses are larger on the nozzle side than on the body side, which is also attributable to the above-mentioned difference in the cross-sectional area. The velocity distributions in **Fig. 9** show some knots in sloshing at the root positions of the ladle's nozzle, causing vibration peaks to appear in the region of 1.30 Hz in the FFT analysis results. The difference in peak frequencies on the body side and the nozzle side appears to be attributable to the flow velocities being increased due to the above-mentioned difference in cross-sectional areas on the body side and on the nozzle side,

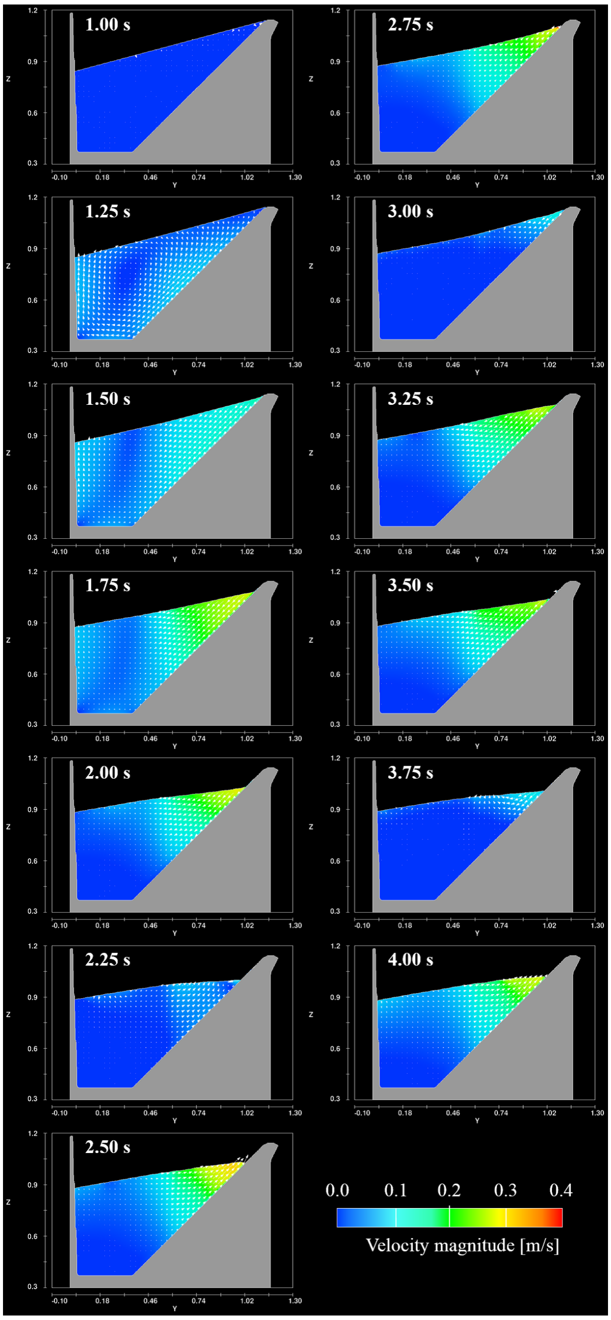

Fig. 9. Color map of velocities (without weir).

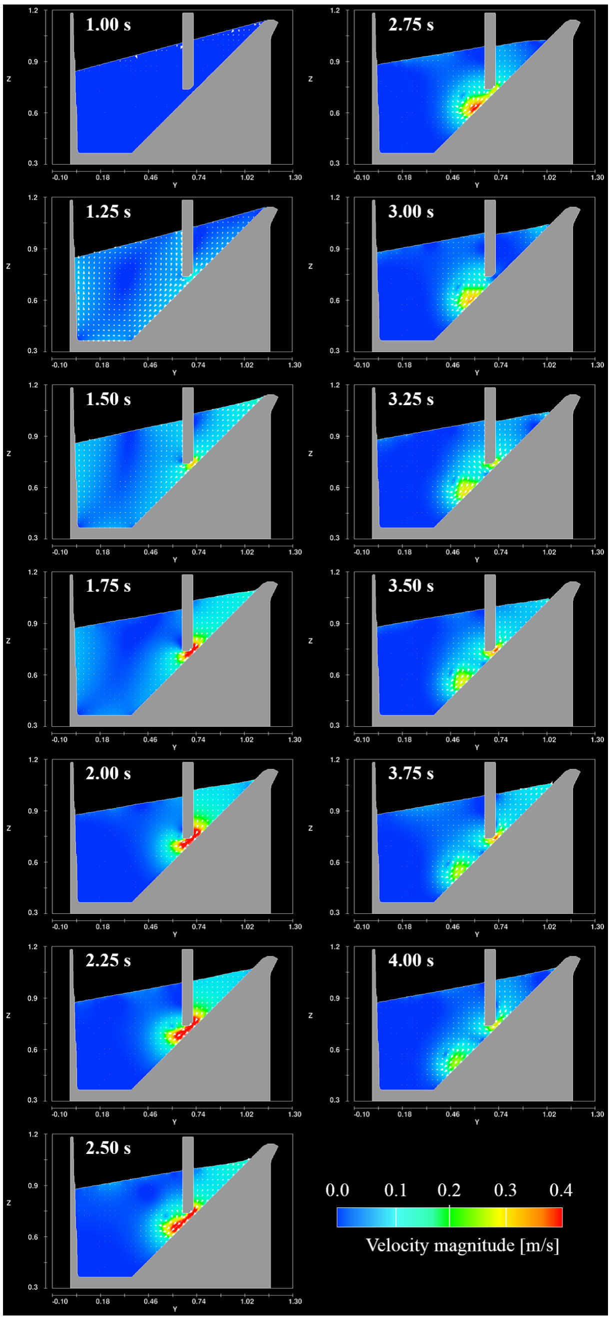

Fig. 10. Color map of velocities (with weir).

shortening the period of vibrations generated on the body side.

For the ladle with a weir, on the other hand, the velocity distributions in **Fig. 10** show significant velocity changes at the weir opening, which do not appear in the ladle without a weir. The measurement of the velocity component in the Y-direction at the weir opening, as shown in **Fig. 6**, shows periodic velocity changes as shown in **Fig. 11**. All of the above seems to suggest that the ladle's backward tilting has caused some volume movement because of the weir opening. Such volume movements elevate and lower the whole liquid surfaces in the tubs on the body side and on the nozzle side, respectively. Residual-volume moving vibrations have a frequency of 0.34 Hz, identical to the peak low frequencies as found by the FFT analysis. Comparatively large frequency peaks other than residual-volume moving vibrations have a frequency of 1.22 Hz, which the motions in the liquid region shown in the velocity distributions show 1st mode sloshing generated on the body side. Frequency peaks of 1.22 Hz are also observed on the nozzle side, which appear to have spread from the vibrations on the body side via the weir opening. Although it was anticipated that sloshing would be excited on the nozzle side as well, neither velocity distributions nor residual vibration waveforms show any sloshing. This was probably because of the small gap between the wall surface on the nozzle side and the weir, which decreases

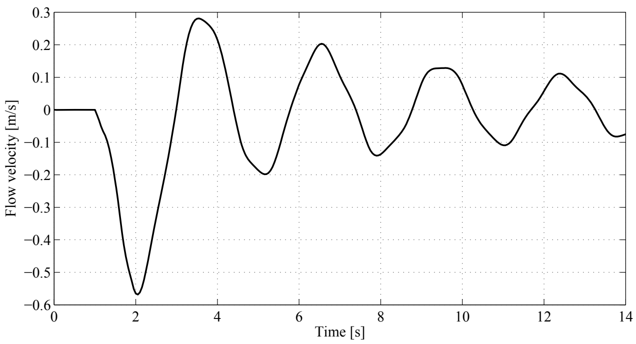

Fig. 11. Flow velocity transients on Y-axis at the weir gate.

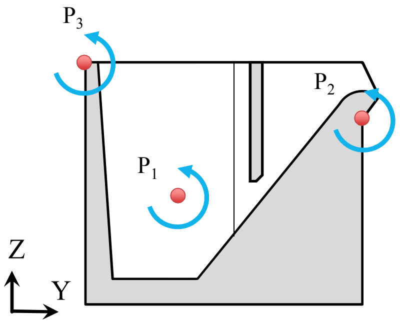

Fig. 12. Center points of tilting motion.

as the liquid level is lowered due to volume movements, and has consequently damped such vibrations.

2.2. Comparison of Center Points of Tilting Motion

Here we discuss differences in flow behaviors at different center points of tilting motion. In order to quantify such differences in flow behaviors, we set the center points of the ladle's tilting motion as shown in **Fig. 12**. P_1 denotes a tilting point near the center of the ladle as described in the preceding section, P_2 a tilting point near the nozzle exit, and P_3 a tilting point on the ladle's top. Of these three tilting points, P_1 and P_2 are the center points of tilting motion to be used in actual system control.

CFD liquid behavior analyses were carried out as in the preceding section, and the FFT analysis results of the residual vibrations on the body side and on the nozzle side are shown in **Fig. 13**, where a marker is attached to the peaks at 0.34 Hz and 1.22 Hz for the sake of easier comparison. The measured frequency responses show that the peak of residual-volume moving vibrations appears at 0.34 Hz and that of the 1st mode vibrations on the body side at 1.22 Hz. This was for all three center points of tilting motion: P_1, P_2, and P_3. In addition, the magnitudes of the peak residual-volume moving vibrations at 0.34 Hz are approximately the same at all three center points. In other words, the center points of tilting motion have no perceivable effect on the volume movement phenomena.

On the other hand, as for the sloshing at 1.22 Hz, there are some distinct differences in the magnitude of the peak 1st mode vibrations, depending on the position of the tilting motion center points. The ladle-tilting motor is often

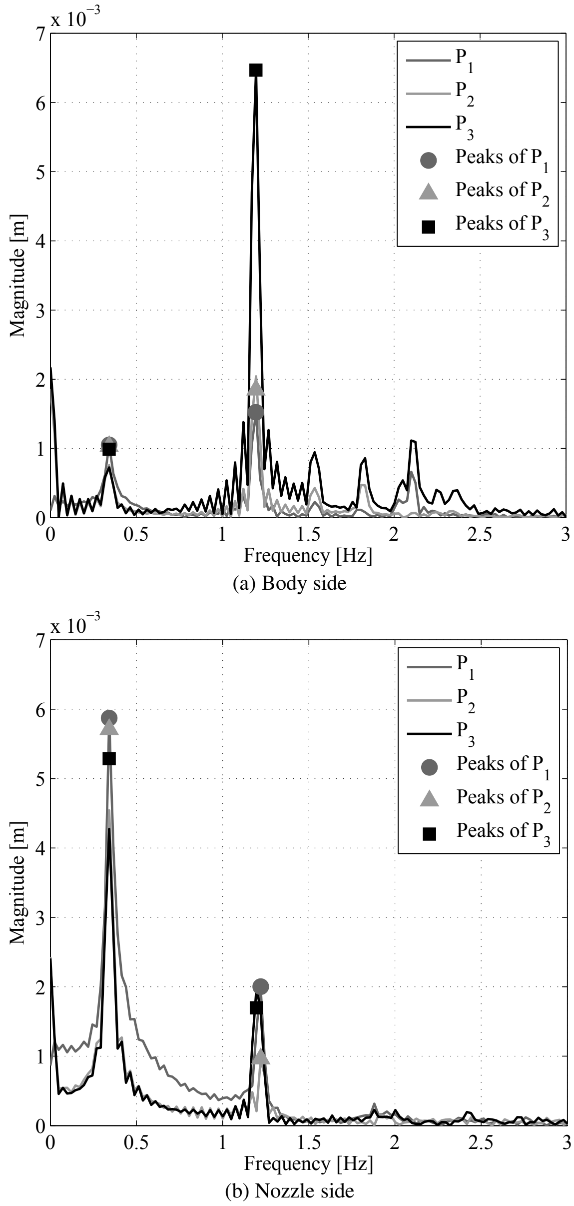

Fig. 13. Frequency peaks of residual vibrations comparing center points of tilting.

mounted at P_1 in consideration of the heavy weight, which includes the molten metal. From a practical consideration it is actually better to position the center point of the tilting motion at P_2, where, when controlling the pouring, the outflowing molten metal's falling trajectory can be better stabilized. In our previous studies we proposed to move the ladle translationally in the Y-direction, as well as vertically, in synchronization with its tilting postures as if P_2 were the center point of the tilting motion [20]. Altering the center point of the tilting motion is equivalent to the above-mentioned synchronous control on the Y- and Z-axes, so it is probably due to the effects of the Y-axial transfer motion, at the time of synchronous control, that the peak vibration of 1.22 Hz with the center point of tilting motion at P_2, has been suppressed by about a half of that with P_1, and sloshing has been more excited with P_3.

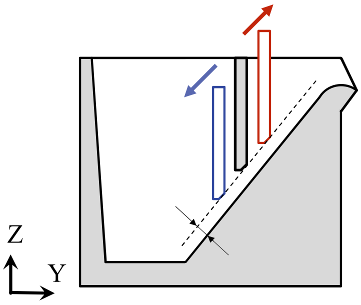

Fig. 14. Variation of weir position.

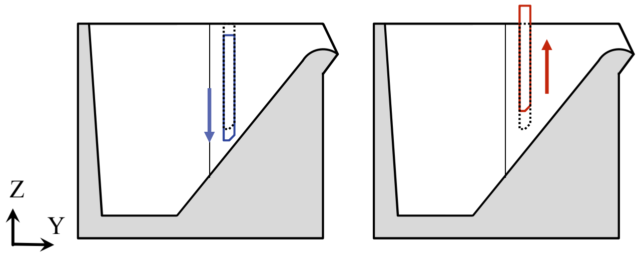

Fig. 16. Variation of weir opening area.

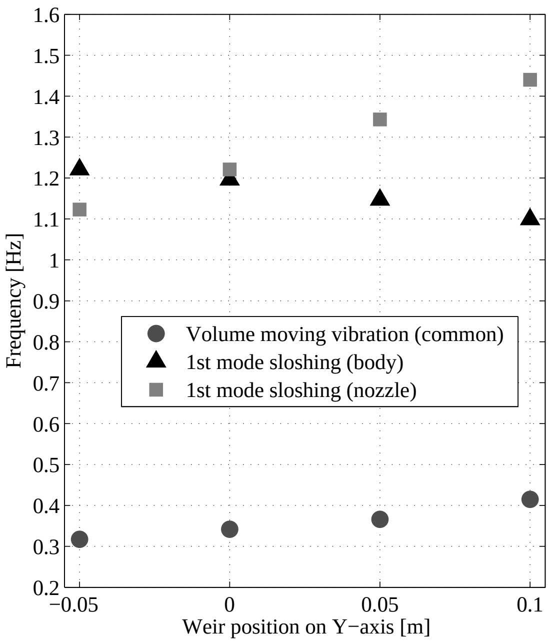

Fig. 15. Peak frequencies at shifted weir positions on Y-axis.

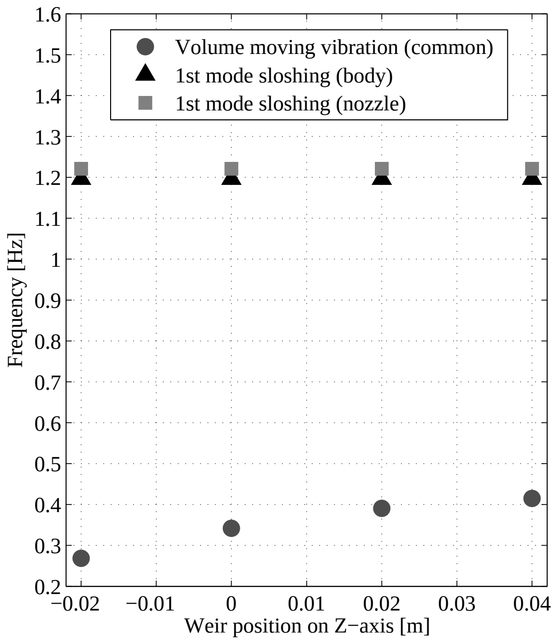

Fig. 17. Peak frequencies shifted weir position on Z-axis.

2.3. Comparison of Different Weir Positions

Here we discuss the cases where the weir is moved to different positions as shown in **Fig. 14**. In particular, we compare the cases of different weir positions between the initial position and positions -0.05 m, $+0.05$ m, and $+0.10$ m from the initial position in the Y-axial direction, while keeping the weir opening area unchanged. The level measuring point on the nozzle side is moved in accordance with the shifted weir positions. Based on the results of FFT analyses of residual vibrations, **Fig. 15** shows the peak frequencies of volume-moving vibrations and the 1st mode sloshing with reference to the different weir positions.

Peak frequencies of volume-moving vibrations on the body side and the nozzle side are similar to each other, but vary with different weir position. As the weir position is moved closer to the nozzle side, the peak frequencies increase, probably due to smaller volumes/cross-sectional areas on the nozzle side which increases the velocity and increases the peak frequency.

As for the 1st mode sloshing in both tubs, the frequencies decrease as the tub gets wider in the Y-direction, and increase when the tub narrows. With the weir in the initial position, the peak frequencies of the 1st mode sloshing on the body side and the nozzle side are approximately the same. Assuming a nearly equal damping ratio, when using the Input Shaping control described below [23, 24], we could target one natural frequency, making it more advantageous from the vibration-suppression control point-of-view if the peak frequency of sloshing in each tub were the same.

2.4. Comparison with Different Weir Opening Areas

Here we discuss the cases where the weir position is shifted upwards and downwards as shown in **Fig. 16**. We compare the cases where the weir opening is positioned at the original height, and where it is shifted by -0.02 m, $+0.02$ m, and $+0.04$ m in the Z-direction. **Fig. 17** shows the transitions of peak frequencies of the volume-moving vibrations and 1st mode sloshing in each tub as done in the preceding section.

The peak frequencies of the 1st mode sloshing are not affected by different opening areas on either the body side or on the nozzle side. On the other hand, the peak frequencies of the volume-moving vibrations increased when the opening area increased, and decreased with smaller opening areas, probably as the opening areas impact the in- and out-flowing volumes per unit time. Despite the weir opening positions only being changed half of the amount of those in the preceding section, the peak frequencies of the volume-moving vibrations changed approximately in the same range, as seen in **Fig. 15**. This suggests that if the opening narrows by solidification of molten metal while using the ladle, it can easily affect the liquid motions inside the ladle.

3. Control of Ladle Motion to Suppress Vibrations

In order to reduce sloshing and volume-moving residual vibrations that are caused by the ladle's backward tilting motion, we elaborate how to shape an appropriate backward tilting velocity input here. This study adopts the input shaping method, a type of feedforward vibration suppression control techniques [23, 24].

3.1. Ladle's Sloshing Suppression Control by Input Shaping Method

We assume that the sloshing and volume-moving residual vibrations can be represented by a linear vibratory system with an acceleration input. Generally, the dynamic characteristics of a linear vibratory system represented by a time-lag system of 2nd order are expressed by the following equation:

$$\ddot{x}+2\zeta\omega_n\dot{x}+\omega_n^2=A\omega_n u \;\; (x\equiv x(t),u\equiv u(t)) \qquad (1)$$

where x is the pendulum's angular displacement, ζ the damping ratio, ω_n the non-damped natural angular frequency, A the proportional gains, and u the input. When an impulse input $u(t)=\delta(t)$ is given at time $t=t_0$, the impulse response can be represented by the following equation:

$$x=\frac{A\omega_n}{\sqrt{1-\zeta^2}}\exp\{-\zeta\omega_n(t-t_0)\}\sin\left\{\sqrt{1-\zeta^2}\omega_n(t-t_0)\right\} \qquad (2)$$

As shown in **Fig. 18**, if the 2nd impulse multiplied by gain K is added to the vibration system with delay time T_d, and a half of the damping natural period with its damping ratio is taken into account, vibrations caused by the 1st and 2nd impulses are cancelled by each other, so that sloshing can be suppressed. Gain K and delay time T_d to be used in the Input Shaping method are expressed as follows on the characteristic parameters of the vibration system.

$$K=\exp\left(-\frac{\zeta\pi}{\sqrt{1-\zeta}}\right),\quad T_d=\frac{\pi}{\omega_n\sqrt{1-\zeta}} \qquad (3)$$

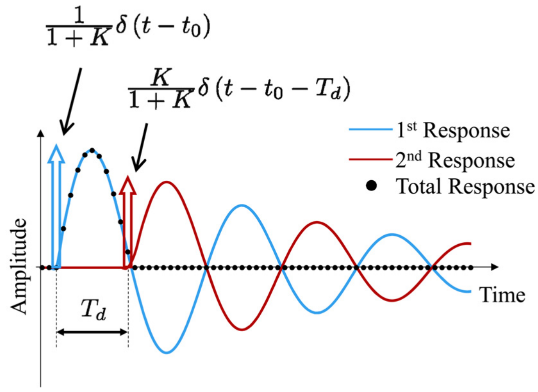

Fig. 18. Input shaping method for impulse input.

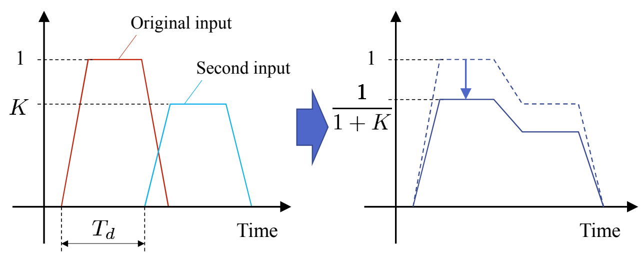

Fig. 19. Input shaping process for trapezoidal shaped input.

As responses to the desired input can be represented by superposing impulse responses, they can also be applied to other-than impulse inputs. **Fig. 19** shows the input shaping method in which they are applied to trapezoidal waveforms to suppress 1st mode vibrations, when a second trapezoidal waveform, K-times as large as the original one, is shaped with a delay T_d and is synthesized with the original one. The input shaping method, in which a new waveform is added to the original velocity waveform, is effective for vibration suppression control but not for positioning control. Therefore by dividing the synthesized waveforms by $(1+K)$, it will be made applicable to such velocity input shaping that can simultaneously do vibration suppression control as well as positioning control.

In this paper, we intend to suppress volume-moving vibrations and 1st mode sloshing on both the body side and the nozzle side. As the natural frequencies of 1st mode sloshing in both tubs are similar, as described in the previous section, we consider that a similar input should be able to suppress sloshing in both tubs. In order to identify the characteristics of the two vibration systems, we have derived design parameters for vibration-suppression control by applying the descent simplex method [25] to the sloshing on the nozzle side of the ladle with a weir for parameter fitting to the time lag system of 2nd order (Eq. (1)). **Table 3** shows the non-damped natural angular frequencies ω_n and damping ratios ζ as obtained by the parameter fitting to sloshing with the center point of tilting motion at P_1, and K and T_d to be used for input shaping by the Input Shaping method.

Table 3. Parameters of Input Shaping control.

	volume-moving vibration	1st mode sloshing
f [Hz]	0.34	1.22
ω_n [rad/s]	2.211	7.672
ζ [-]	0.073	0.009
K [-]	0.788	0.972
T_d [s]	1.476	0.411

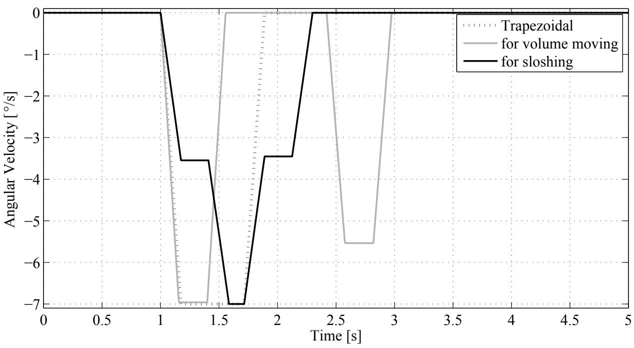

Fig. 20. Designed velocity based on Input Shaping method for 1 mode vibration.

3.2. Input Shaping Control for Individual 1 Mode Vibrations

Let us first discuss the case of providing individual control inputs to volume-moving vibrations and 1st mode sloshing. **Fig. 20** shows the trapezoidal input with no control and the Input Shaping input for volume-moving vibrations and 1st mode sloshing as designed with the parameters obtained in Section 3.1. We have adjusted the original trapezoidal input to be used for designing the Input Shaping input so that the Input Shaping input should result in the same maximum angular velocity of $-7°$/s as the trapezoidal input with no control. **Fig. 21** shows the frequency responses as obtained by the FFT analyses of generated residual vibrations. We have attached markers to indicate the peak frequency responses in the region of 0.34 Hz and 1.22 Hz.

From **Fig. 21(b)** it can be seen, more clearly than in **Fig. 21(a)**, that the Input Shaping control has reduced the peak frequency response of volume-moving vibrations at 0.34 Hz to 50% or less than that of the trapezoidal input, and has doubled the peak velocity of the trapezoidal input at 1.22 Hz. As the period of volume-moving vibrations is approximately an integer multiple of the 1st mode sloshing period, both vibrations appeared to have sympathetically vibrated to move the peak value upward.

On the other hand, Input Shaping control of 1st mode sloshing has not significantly changed the peak value at 0.34 Hz, equivalent to the volume-moving vibrations, but has substantially reduced the peak value at 1.22 Hz.

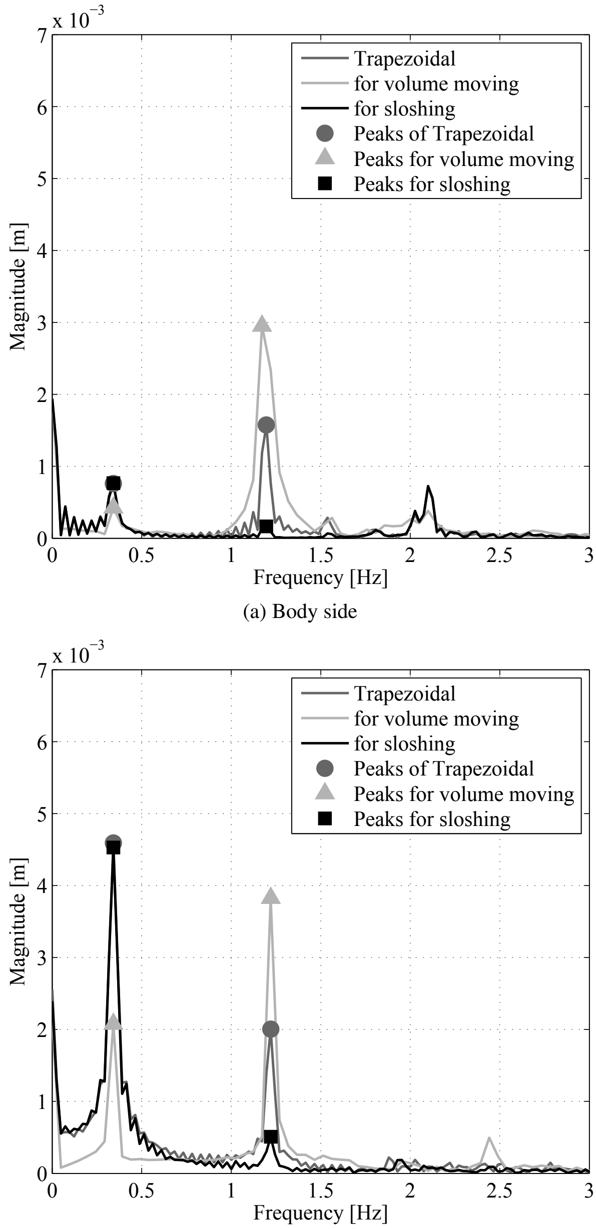

(a) Body side

(b) Nozzle side

Fig. 21. Frequency responses with applied input shaping control.

3.3. Input Shaping Control of 2 Mode Vibrations and Stopping Point for Backward Tilting Motion

Lastly, we discuss the case of suppressing two vibration modes: volume-moving vibrations and 1st mode sloshing. If you want to suppress n vibration modes by the Input Shaping method, you need to synthesize 2^n times the input after taking into account the vibration frequencies and damping ratios of each vibration mode [23, 24]; in this study, we have synthesized four waveforms. **Fig. 22** shows the trapezoidal input I and the designed 2 mode Input Shaping input. We have adjusted the original trapezoidal waveform so as to make the inputs have an approximately $-7°$/s maximum angular velocity. In order to eval-

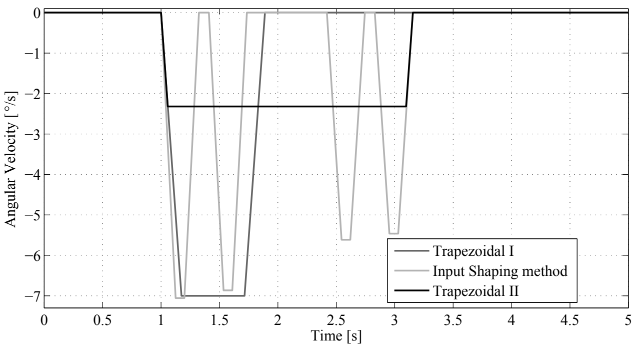

Fig. 22. Designed velocity based on Input Shaping method for 2 mode vibrations.

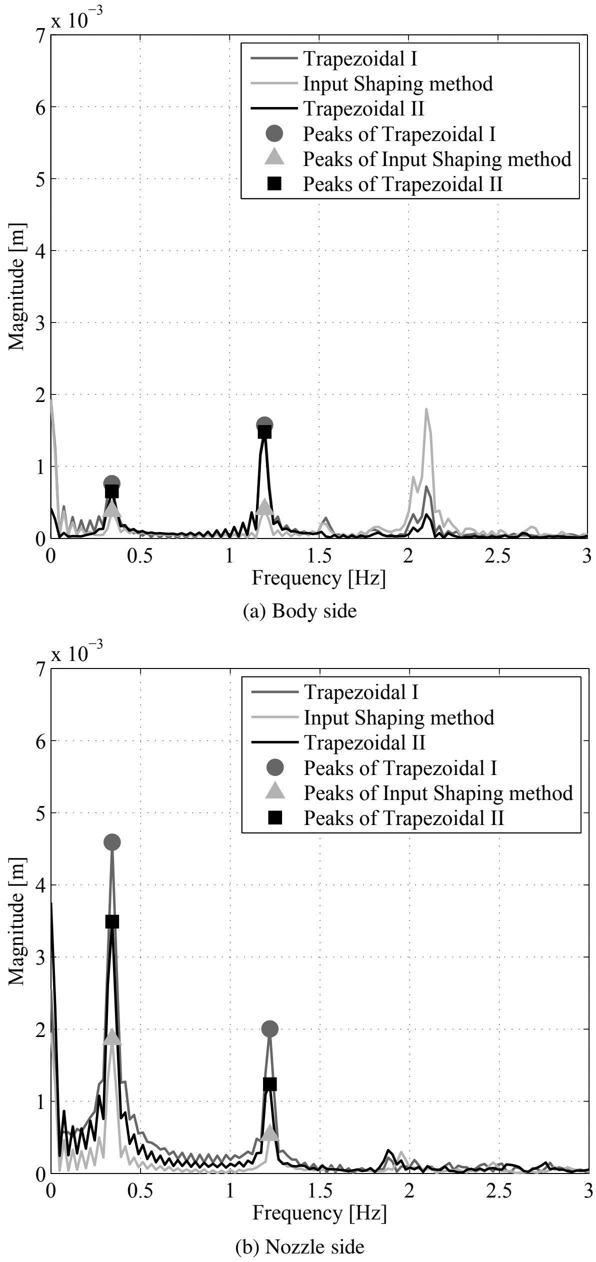

Fig. 23. Frequency responses from applied Input Shaping control.

uate the time required for the backward tilting motion, we have designed trapezoidal input II that ends the motion at the same time as the 2 mode input-shaping input and have compared them.

Figure 23 shows the frequency responses as obtained from the FFT analyses of residual vibrations, and **Figs. 24** and **25** the time response graphs for the Input Shaping inputs and the trapezoidal input I and for the Input Shaping input and the trapezoidal input II, respectively. Unlike in **Fig. 21** for individual vibrations, they show that the peak frequency responses with 2 mode Input Shaping input have decreased at both 0.34 Hz and 1.22 Hz as compared with those of the trapezoidal input I. Comparison with the results of the trapezoidal input II that ends the backward tilting motion in the same time as for the 2 mode Input Shaping input, shows the both peaks have become smaller, which proves vibration suppression control has been achieved in the same backward tilting time.

The peaks in the neighborhood of 2.1 Hz in **Fig. 23(a)** are for the 2nd mode sloshing and are not in the scope of control of this study, and it appears that the Input Shaping input has moved them upward. They are expected to be suppressed together with other vibrations by shaping 3 mode Input Shaping input by the above-mentioned method.

4. Conclusion

In this paper, regarding an automatic tilting-type molten-metal pouring system used in the casting industry, and in particular ladles with weirs that are used in actual molten-metal pouring processes, we have analyzed fluid behaviors and sloshing generated inside a ladle with a weir when it is tilted backward in the same way as a conventional weir-less ladle. The analytic results show that sloshing as well as residual vibrations due to fluid volume movements via the weir opening are generated in a ladle with a weir.

We studied tilted ladles with weirs placed backwards, with different center points of backward tilting, and found that peak frequencies of generated vibrations remain unchanged but vibration amplitudes have changed with different center points. In addition, we have confirmed that peak frequencies are affected by weir positions and opening areas, which suggests that optimum vibration characteristics can be provided by weir design.

Lastly, we have demonstrated that volume-moving residual vibrations and 1st mode sloshing on the body side of a ladle can be substantially reduced by shaping their backward tilting velocity waveforms by the Input Shaping method, one of the feedforward vibration suppression control approaches.

In the future, we plan to study vibration characteristics of a ladle in other postures, and verify the effectiveness of the analytic results described in this paper by representing them by a simpler mathematical model, as well as by experiments on an actual molten pouring system.

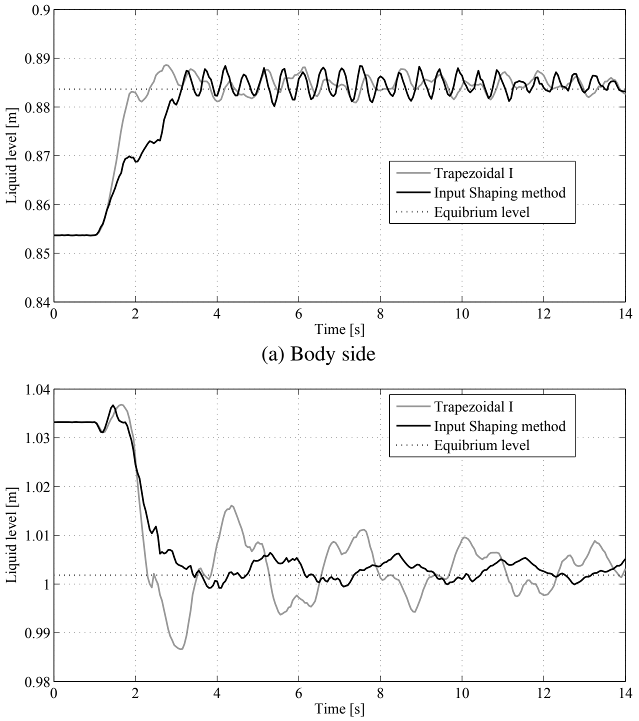

(a) Body side

(b) Nozzle side

Fig. 24. Residual vibrations of trapezoidal I and Input Shaping method.

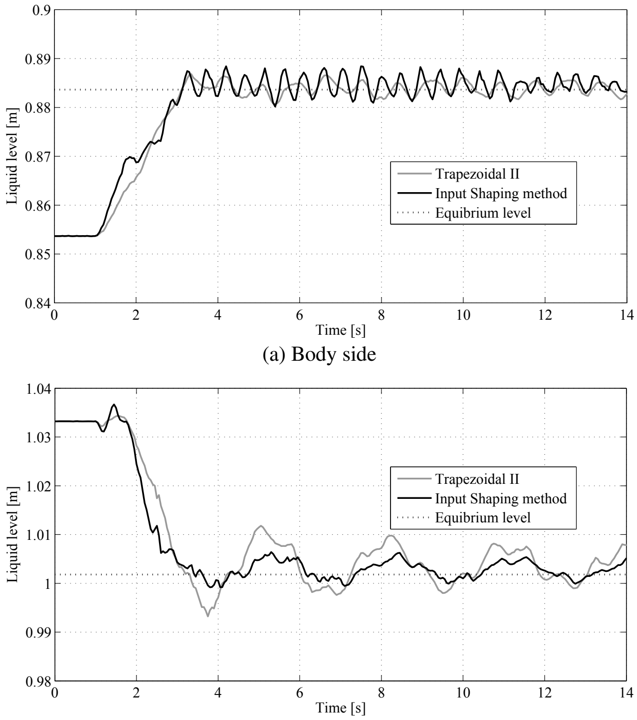

(a) Body side

(b) Nozzle side

Fig. 25. Residual vibrations of trapezoidal II and Input Shaping method.

References:

[1] W. Lindsay, "Automatic pouring and metal distribution systems," Foundry Trade J., February 10, pp. 151-176, 1983.

[2] K. Terashima, "Recent Automatic Pouring and Transfer System in Foundries," SOKEIZAI, Vol.39, No.1, 1998.

[3] E. Neuman and D. Trauzeddel, "Pouring Systems for Ferrous Applications," Foundry Trade J., July, pp. 23-24, 2002.

[4] Y. S. Lerner, "Ironing Out the Pouring Options," Modern Casting, Vol.93, No.11, p. 44, 2003.

[5] Y. Noda and K. Terashima, "Modeling and Feedforward Flow Rate Control of Automatic Pouring System with Real Ladle," J. Robot. Mechatron., Vol.19, No.2, pp. 205-211, 2007.

[6] Y. Noda and T. Nishida, "Precision Analysis of Automatic Pouring Machines for the Casting Industry," Int. J. Automation Technol., Vol.2, No.4, pp. 241-246, 2008.

[7] S. Paranjape and P. D. Chaubal, "Automatic Pouring Systems Boosts Output at Mahindra Hinoday Ind," Metalworld, June 2010, pp. 24-27, 2010.

[8] V. I. Dubodelov, V. K. Pogorsky, and M. S. Goryuk, "Magnetodynamic Mixer-Batcher for Overheating and Pouring of Cast Iron," Proc. 9th Int. Symposium on Science and Processing of Cast Iron, pp. 481-486, 2009.

[9] M. Grundelius and B. Bernhardsson, "Control of liquid slosh in an industrial packaging machine," Proc. of IEEE Int. Conf. on control applications, pp. 1654-1659, 1999.

[10] H. Takahara, S. Tamura, J. Fukuda, Y. Hikita, and K. Kimura, "Free Vibration Analysis of Multi-Surface Liquid Motion in a Rectangular Tank with Different Surface Areas," J. of Environment and Engineering, Vol.6, No.2, pp. 340-351, 2011.

[11] H. Takahara, K. Hara, and T. Ishida, "Nonlinear liquid oscillation in a cylindrical tank with an eccentric core barrel," J. of Fluids and Structures, Vol.35, pp. 120-132, November 2012.

[12] H. Katsube and M. Nagai, "Study of Liquid Surface Wave Control of an Incline-Type Automatic Pouring Machine (1st Report, Modeling and Control)," Trans. Jpn. Soc. Mech. Eng. Ser. C, Vol.65, No.634, pp. 2345-2351, 1999.

[13] H. Katsube and M. Nagai, "Study of Liquid Surface Wave Control of an Incline-Type Automatic Pouring Machine (2nd Report, Proposal of Preview Control by Rotation on Transfer)," Trans. Jpn. Soc. Mech. Eng. Ser. C, Vol.67, No.658, pp. 1792-1798, 2001.

[14] H. Katsube and M. Nagai, "Study of Liquid Surface Wave Control of an Incline-Type Automatic Pouring Machine (3rd Report, Cooperative Control of Incline Control and Liquid Surface Control)," Trans. Jpn. Soc. Mech. Eng. Ser. C, Vol.68, No.670, pp. 1747-1752, 2002.

[15] K. Kanazawa, K. Yano, and T. Nakada, "Motion Curve Optimization Method Based on Genetic Algorithm and Its Application to Bottling Machines," Trans. of the Society of Instrument and Control Engineers, Vol.49, No.1 pp. 158-165, 2013.

[16] R. Shibuya, Y. Noda, Y. Maeda, and K. Terashima, "Estimation of Natural Frequency and Suppression Control of Sloshing during Ladle Transfer and Tilt Motion by Automatic Pouring Machine," J. of Japan Foundry Engineering Society, Vol.86, No.1, pp. 12-18, 2014.

[17] R. Fukushima, Y. Noda, and K. Terashima, "Falling Position and Anti-Sloshing Control of Liquid Using Automatic Pouring Robot," Proc. of Int. Ph.D. Foundry Conf., pp. 45-55, 2009.

[18] K. Terashima and K. Yano, "Sloshing analysis and suppression control of tilting-type automatic pouring machine," Control Engineering Practice, Vol.9, pp. 607-620, 2001.

[19] J. Thielke, "Automatic Pouring Systems," ASM Metals Handbook, Vol.15, 2002.

[20] K. Terashima, K. Yano, Y. Sugimoto, and M. Watanabe, "Position Control of Ladle Tip and Sloshing Suppression during Tilting Motion in Automatic Pouring Machine," Proc. 10th IFAC symposium on Automation in Mining, Mineral and Metal Processing, Japan, pp. 182-187, 2001.

[21] C. W. Hirt, "SOLA-A Numerical Solution Algorithm for Transient Fluid Flows," Los Alamos Science Laboratory Report, LA-5852, 1975.

[22] C. W. Hirt, "Identification and Treatment of Stiff Buble Problems," Technical Note, Vol.35, 1992.

[23] N. C. Singer and W. P. Seering, "Preshaping Command Inputs to Reduce System Vibration," J. of Dynamic Systems, Measurement, and Control, Vol.112, No.1, pp. 76-82, 1990.

[24] W. Aribowo and K. Terashima, "Cubic Spline Trajectory Planning and Vibration Suppression of Semiconductor Wafer Transfer Robot Arm," Int. J. Auto. Tech., Vol.8, No.2, pp. 265-274, 2014.

[25] J. A. Nelder and R. Mead, "A simplex method for function minimization," Comp. J., Vol.7, No.4, pp. 308-313, 1965.

Name:
Atsushi Ito

Affiliation:
Ph.D. Candidate, Department of Mechanical Engineering, Toyohashi University of Technology

Address:
1-1 Hibarigaoka, Tempaku, Toyohashi, Aichi 441-8580, Japan

Brief Biographical History:
2012 Received B.Eng. degree in Production System Engineering from Toyohashi University of Technology
2014 Received M.Eng. degree in Mechanical Engineering from Toyohashi University of Technology

Main Works:
• high speed and high accuracy control of automatic pouring machine in casting industry

Membership in Academic Societies:
• Society of Instrument and Control Engineers (SICE)
• Japan Foundry Engineering Society (JFS)
• Japan Society of Mechanical Engineering (JSME)
• Robotics Society of Japan (RSJ)

Name:
Ryosuke Tasaki

Affiliation:
Assistant Professor, Department of Mechanical Engineering, Toyohashi University of Technology

Address:
1-1 Hibarigaoka, Tempaku, Toyohashi, Aichi 441-8580, Japan

Brief Biographical History:
2006 Received B.S. degree in Mechanical Engineering from Kyoto Institute of Technology
2008 Received M.S. degree in Production System Engineering from Toyohashi University of Technology
2011 Received Ph.D. degree in Electric and Information Engineering from Toyohashi University of Technology
2012- Assistant Professor, Department of Mechanical Engineering, Toyohashi University of Technology

Main Works:
• industrial process automation, mechanical dynamics control, robotics

Membership in Academic Societies:
• Society of Instrument and Control Engineers (SICE)
• Japan Foundry Engineering Society (JFS)
• Japan Society of Mechanical Engineering (JSME)
• Institute of Electrical and Electronics Engineers (IEEE)

Name:
Makio Suzuki

Affiliation:
Sintokogio, Ltd.

Address:
3-1 Honohara, Toyokawa, Aichi, 442-8505, Japan

Brief Biographical History:
1996 Received B.S. degree in Production System Engineering from Toyohashi University of Technology
1998 Received M.S. degree in Production System Engineering from Toyohashi University of Technology
2002 Received Ph.D. degree in Electric and Information Engineering from Toyohashi University of Technology
2001- Sintokogio, Ltd.

Main Works:
• Pouring control of automatic pouring machine in casting industry
• Pressure control of electric actuator
• Suppression control of crane
• Pressure control of roll press
• Sequence control of dust collector

Membership in Academic Societies:
• Japan Society of Mechanical Engineering (JSME)
• Robotics Society of Japan (RSJ)

Name:
Kazuhiko Terashima

Affiliation:
Professor, Department of Mechanical Engineering, Toyohashi University of Technology

Address:
1-1 Hibarigaoka, Tempaku, Toyohashi, Aichi 441-8580, Japan

Brief Biographical History:
1981 Ph.D. at Precision Mechanics of Kyoto University
1982- Assistant Professor and Associate Professor, Toyohashi University of Technology
1991-1992 Visiting Researcher, Techinische Universitat Munchen
1994- Professor, Toyohashi University of Technology

Main Works:
• "Hybrid Impedance Control of Massage Considering Dynamic Interaction of Human and Robot Collaboration Systems," J. of Robotics and Mechatronics, Vol.21, No.1, pp. 46-15, 2009.
• "Supervisory Control of Automatic Pouring Machine," Control Engineering Practice, Elsevier, Vol.18, No.3, pp. 230-241, 2010.
• "Medical Round Robot – Terapio –," J. of Robotics and Mechatronics, Vol.26, No.1, pp. 112-114, 2014.

Membership in Academic Societies:
• Institute of Electrical and Electronics Engineers (IEEE)
• Society of Instrument and Control Engineers (SICE)
• Japan Society of Mechanical Engineering (JSME)
• Japan Foundry Engineering Society (JFS)